Proceedings of the 17th
IEEE International Conference on Nanotechnology
Pittsburgh, USA, July 25-28, 2017

Piezoelectric Response of Graphene-Filled PVDF Nanocomposites Through Piezoresponse Force Microscopy (PFM)

M. Fortunato, H.C. Bidsorkhi, G. De Bellis, *Member, IEEE,* F. Sarto, and M.S. Sarto, *Fellow, IEEE*

***Abstract*— The piezoelectric properties of Poly(vinylidene fluoride) (PVDF) mainly depend on its most polar *β*-phase. In this work, we investigated through Piezoresponse Force Microscopy (PFM) the piezoelectric properties of PVDF composite films when we induce the formation of *β*-phase crystals adding graphene nanoplatelets (GNPs) without any chemical modification or poling. At first, we fabricated GNP-filled PVDF composite films by the solution casting method. Then, we investigated the piezoelectric response of different samples: neat PVDF, PVDF-based nanocomposites filled with 0.3 wt%, 0.5 wt% and 0.7 wt% GNPs . The morphology of the produced PVDF/GNP composites was investigated through field-emission scanning electron microscopy (FE-SEM) and atomic force microscopy (AFM). The *β*-phase formation was assessed through Fourier transform infrared spectroscopy (FT-IR) measurements.**

I. Introduction

Poly(vinylidene fluoride) [PVDF; $(CH_2CF_2)_n$] is a semi-crystalline and ferroelectric polymer. Due to its chemical resistance, thermal stability, high mechanical strength, large remnant polarization, short switching time, and peculiar electrical properties, PVDF has attracted, in recent years, attention for its emerging application in organic electronics, biomedical, optoelectronics and energy harvesters [1-3]. In PVDF the amorphous and crystalline phases coexist. Several crystalline phases can be identified in PVDF (*α*-, *β*-, *γ*-, and *δ*-phase). The *α*-phase is non-polar and it is the most stable polymorph when PVDF is directly cooled down from the molten state. The *β*-phase exhibits the strongest ferro-, piezo-, pyroelectric properties, due to its largest spontaneous polarization ($7x10^{-30}$ Cm) [4]. This phase is generally obtained through uniaxial or biaxial stretching of melt-crystallized films [5], melt crystallization under high pressure [6], crystallization from solution under special condition [7] or through the application of high electric fields to PVDF in its *α*-phase [8]. Depending on the processing route, *β*-PVDF can be obtained in a porous or non-porous form [9]. Several studies have also demonstrated that the addition modified carbon nanotubes (CNTs) [10], modified GNPs [11], [12] or clay particles can induce *β*-phase formation in PVDF nanocomposites obtained by solution casting. The aim of the present work is to investigate the piezoelectric properties of composite films made of PVDF filled with unmodified and un-functionalized GNPs through Piezoresponse Force Microscopy (PFM) and to correlate the piezoelectric response of the samples with the induced *β*-phase as revealed through Fourier transform infrared spectroscopy (FT-IR) measurements. Indeed, the PFM, is a very effective technique to characterize the piezo electric properties of materials at the nanoscale. The PFM is able to study the local sample strain generated by the applied electrical field with a lateral resolution of a few nanometers [13, 14]. PFM is a versatile and non-invasive method to investigate the piezoelectric response of the ferroelectric material without an elaborate sample preparation. PFM investigations have been adopted to assess the piezoelectric properties of the PVDF/GNP nanocoposites at the nanoscale. The morphology of the produced samples was investigated through high-resolution field-emission scanning electron microscopy (FE-SEM) and atomic force microscopy (AFM). *β*-phase formation was assessed through FT-IR measurements.

M. Fortunato, H.C. Bidsorkhi, G. De Bellis and M.S. Sarto are with the Department of Astronautical, Electrical and Energy Engineering (DIAEE), Sapienza University of Rome, Via Eudossiana 18, Rome, 00154 Italy and Research Center for Nanotechnology applied to Engineering (CNIS), Sapienza University of Rome, Piazzale Aldo Moro 5, Rome, 00185 Italy (corresponding author: +390644585528 e-mail: marco.fortunato@uniroma1.it).

F. Sarto is with, ENEA, Frascati Research Center, Via Enrico Fermi, 45, Frascati, Rome, Italy

II. Materials and Methods

A. Production of PVDF/GNP film composites

Neat PVDF film was fabricated via a solution mixing method. PVDF was firstly dissolved in N,N-dimethylformamide (DMF), the preferred solvent for PVDF, through 2 hours-magnetic stirring at 65 °C. Then, the obtained mixture was casted onto a glass plate and cured in oven for 8 hours at 80 °C, as sketched in Figure 1.

GNPs were produced through thermal expansion of a graphite intercalation compound (GIC) [15]. The declared mean lateral size of GIC is 350 μm. GIC underwent a thermal shock driven expansion in air at 1150°C for ~ 5 sec, increasing its volume by roughly 200 times, obtaining worm like expanded graphite, also called thermally expanded graphite oxide (TEGO).

The GNP/PVDF nanocomposite films were fabricated via a solvent-mediated technique [16]. PVDF was firstly dissolved in N,N-dimethylformamide (DMF), the preferred solvent for PVDF, through 2 hours-magnetic stirring at 65 °C. Then, TEGOs were added in a PVDF-DMF solution, and the obtained colloidal suspension was tip sonicated using an ultrasonic processor in pulsed mode for 20 minutes. The obtained mixture was casted onto a glass plate and cured in oven for 8 hours at 80 °C, as sketched in Fig. 2.

The concentrations of the produced GNP/PVDF nanocomposite films were 0.3 wt%, 0.5 wt% and 0.7 wt%. The obtained films, having thickness of approximately 30 μm, were peeled off the substrate.

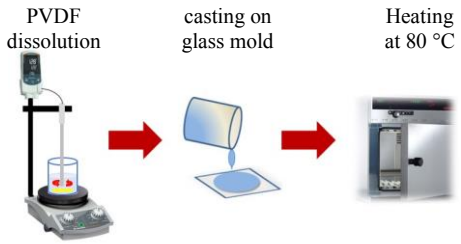

Figure 1 Preparation route of the neat PVDF sample.

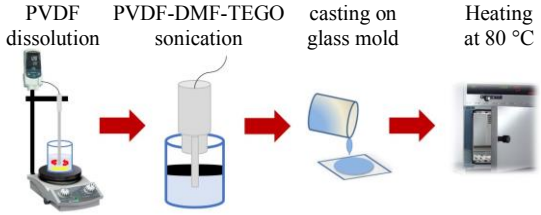

Figure 2. Preparation route of the PVDF/GNP samples.

B. Scanning Electron Microscopy Characterization

The morphology of the produced samples was observed using Field Emission Scanning Electron Microscopy (FE-SEM, Zeiss Auriga) operated at an accelerating voltage of 5 kV. Prior of the SEM imaging, the produced samples were sputter coated (Quorum Q150T ES) with a homogenous Cr layer 30 nm of thickness varying between 20 nm 30 nm, respectively for nanocomposite filled with 0.5 wt% or 0.7 wt% GNPs and for the neat PVDF and nanocomposites filled with 0.3 wt% GNPs.

C. FTIR analysis

The FT-IR system was a single-beam instrument (Bruker Tensor 27), equipped with a room temperature deuterated triglycine sulfate (DTGS) detector, mid-IR source and a KBr beamsplitter. Spectra were acquired in the range 4000-600 cm-1 with resolution of cm^{-1}.

Samples were analyzed in the attenuated total reflection (ATR) configuration, using the Pike Miracle ATR cell equipped with a Diamond/ZnSe crystal, with a sampling area of 6 mm diameter.

D. Piezoresponse Force Microscopy (PFM) Characterization

The piezoelectric response was evaluated using PFM (Dimension Icon, Bruker-Veeco). This technique is based on the standard contact mode AFM setup [14]. In addition to the AFM setup, an alternating voltage is applied to the sample and the tip is grounded. In this work, the PFM measurements were performed under the following conditions: silicon cantilever (Bruker) with nominal spring constant 5 N/m, resistivity: 0.01-0.025 Ωcm, nominal resonance frequency 150 kHz. The samples were glued on a metal plate by silver paint. In order to measure the piezoresponse of the samples, an a.c. voltage was applied with amplitude from 0 V to 10 V, in 2 V-steps and a frequency of 20 kHz. Scan rate was 0.5 Hz and the scan area was (500×500) nm^2. The dimension of the scan area was selected considering that the PVDF films have a porosity in the range of tens of microns. The scope is to perform a local characterization of the piezoelectric response of the material and avoiding that the topography signal interferes with the PFM measurement.

III. Results and Discussions

A. Morphology

FE-SEM image of neat PVDF are shown in Figs. 3(a) and (b). The surface is characterized by a spherulitic structure with porosity in the micrometric range. When GNP were added, a similar spherulitic structure was observed as well as a good integration between GNPs and the polymer matrix; in fact, GNPs appear markedly embedded into the PVDF metrix. Figs. 3(d), (f) and (h) show the details of GNPs emerging from the surface of the composite films and partially covered by the polymer matrix at 0.3 wt%, at 0.5 wt% and at 0.7 wt%, respectively. Figs. 3(c), (e) and (g) show the FE-SEM micrographs of PVDF/GNP films at 0.3 wt%, at 0.5 wt% and at 0.7 wt%, respectively.

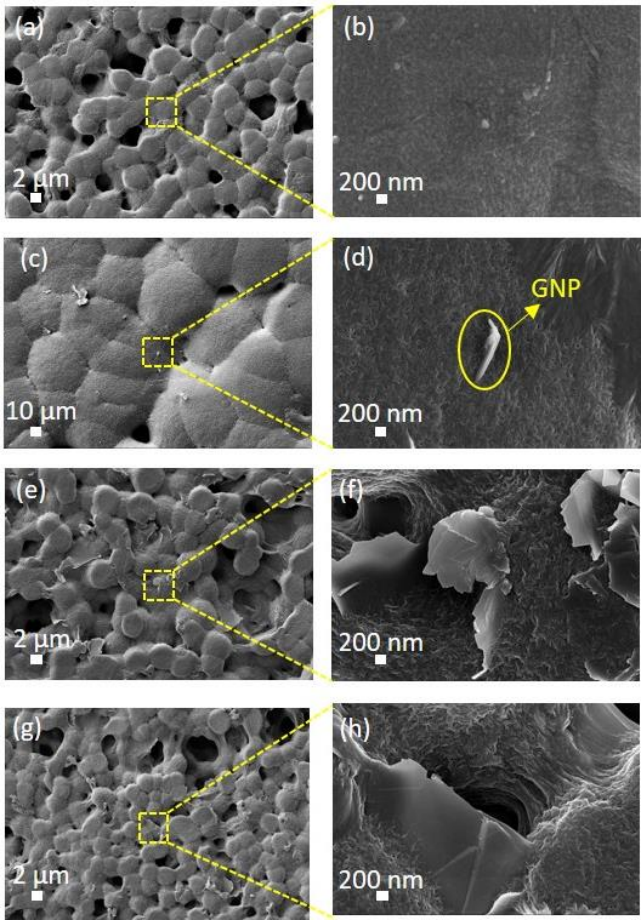

Figure 3 FE-SEM images of neat PVDF at low magnification (a) and at high magnification (b), PVDF/GNP nanocomposite with 0.3 wt% at low magnification (c) and at high magnification (d), PVDF/GNP nanocomposite with 0.5 wt% at low magnification (e) and at high magnification (f) and PVDF/GNP nanocomposite with 0.7 wt% at low magnification (g) and at high magnification (h).

We observed that the dimensions of the spherulites decrease as the GNP concentration increases, as described in [16]. The average values of the spherulite diameter, estimated from the FE-SEM images, are reported in Table 1.

Table 1 Average values of the spherulite diameter estimated from FE-SEM images.

Sample	Spherulite's diameter (µm)
Neat PVDF	4.87 ± 0.97
PVDF/GNP 0.3 wt%	38.80 ± 14.44
PVDF/GNP 0.5 wt%	5.00 ± 0.95
PVDF/GNP 0.7 wt%	4.13 ± 0.20

B. *FT-IR Analysis*

The existence of the β-phase in the PVDF/GNP nanocomposites was investigated using FT-IR spectroscopy. The characteristic peaks attributed to the FT-IR absorbance band of α-phase are located at 1423, 1383, 120, 1147, 976, 855, 795 and 763 cm^{-1} [17]. The electroactive polar β-phase can be clearly identified from the peaks at 1275 cm^{-1} and 840 cm^{-1}, whereas the semi-polar γ-phase is evident from the peak at 1234 cm^{-1} [18], [19].

All of our samples showed the presence of the electroactive phase, evinced through the characteristic γ peak at 1234 cm^{-1} and β peak at 840 cm^{-1} (Fig. 4).

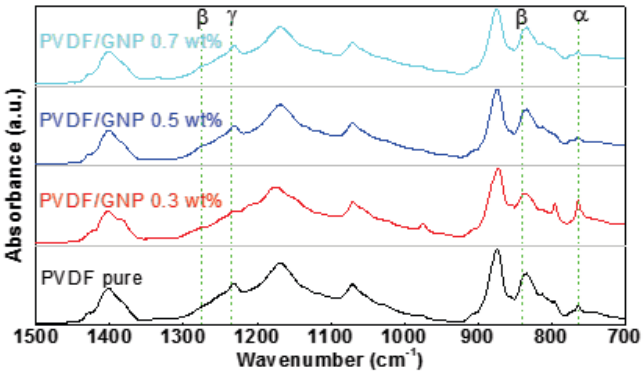

Figure 4 FT-IR spectra of neat PVDF and PVDF/GNP nanocomposites.

The FT-IR measurements weare used to evaluate the fraction of the electroactive β-phase of PVDF, by using the following equation [20]:

$$F(\beta) = \frac{A_\beta}{(K_\beta / K_\beta)A_\alpha + A_\beta} \quad (1)$$

where $F(\beta)$, represents the β-phase content; A_α and A_β the absorbance at 766 and 840 cm^{-1}, respectively; K_α and K_β are the absorption coefficient at the respective wavenumbers, which values are 6.1 x 10^4 and 7.7 x 10^4 cm^2mol^{-1}, respectively. The obtained values are reported in Table 2.

Table 2 Relative fraction of the β-phase estimated from FT-IR spectra.

Sample	$F(\beta)$
Neat PVDF	0.687
PVDF/GNP 0.3 wt%	0.481
PVDF/GNP 0.5 wt%	0.647
PVDF/GNP 0.7 wt%	0.615

C. *Piezoelectric response*

The PFM technique is based on the standard contact mode AFM setup. In addition, an alternating voltage is applied to the sample. The cantilever detects the deformation of the material, through the photodiode. In order to separate the topography and piezoresponse signal, a lock-in amplifier (LIA), which also acts as a sharp band pass filter, is required. The LIA compares the response signal with the reference signal and amplifies only the frequency component that is equal to the reference signal. Since the reference signal and the voltage applied to the tip have the same frequencies, the expected piezoresponse is also at the same frequencies. This allows measurements with a high signal-to-noise ratio even for small signals, like average displacements of just a few picometers (pm). The raw amplitude signal measured using the quadrant photodiode and lock-in amplifier is then converted to a displacement amplitude measurement using a calibration factor.

In Fig. 5 the three-dimensional topography and the piezoelectric contrast, scanning an area of (500×500) nm^2, are reported. As we can see the piezoelectric contrast does not directly correlate with the topography, indicating that the β-phase domains are not related to the morphology of the films [21]. Therefore, we can say that the piezoelectric effect is due to intrinsic piezoelectric properties of the materials and not originated from the cross-talk with the topography. This is in agreement with the results reported for PVDF by Serrado Nunes et al. [21], showing that the piezoelectric constant does not directly follow the topographic shape.

In order to evaluate the average piezoelectric properties of the samples we performed the PFM measurements on 19 different regions for each sample (scanning area (500×500) nm^2). In Fig. 6 we report the average values of displacement, obtained from all measurements, as a function of the amplitude of the applied a.c. voltage.

As we can see, we obtained a very good linear behavior of the piezoelectric response as a function of the applied voltage, in agreement with the theory of the converse piezoelectric effect. In fact, according to Eq. (2) the displacement (Δz) depends linearly upon the applied voltage amplitude (V_{ac}) and the angular coefficient is the piezoelectric coefficient (d_{ij}):

$$d_{ij} = \Delta z / V_{ac} \quad (2)$$

In our experimental conditions the voltage is applied along the vertical axis, so that the measured piezoelectric coefficient is d_{33}. We estimated the value of d_{33} of the PVDF/GNP nanocomposite films using as reference sample the periodically poled lithium niobate (PPLN), purchased from Bruker. Since the piezoelectric coefficient in the PPLN sample is known (d_{33} = 7.5 pm/V), it is possible to determine the calibration parameter ξ, from the slope of the piezoresponse amplitude vs applied voltage, using the following equation:

$$A_{piezo} = \xi d_{33} V_{ac} \quad (3)$$

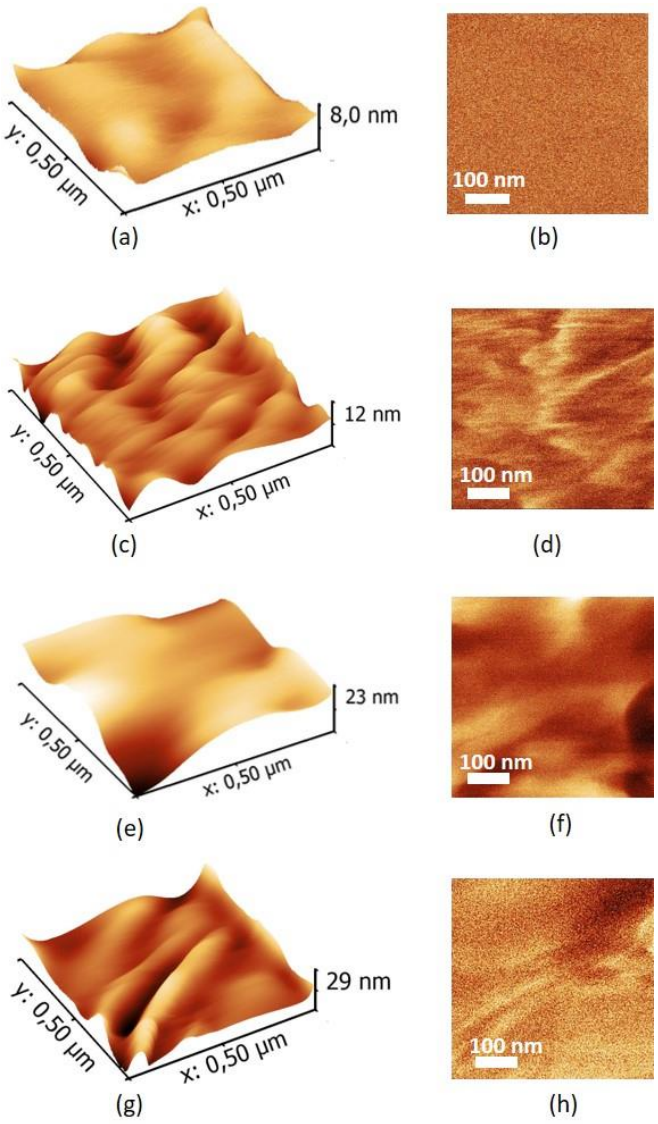

Figure 5 Three-dimensional topography of neat PVDF (a), PVDF/GNP at 0.3 wt% (c), PVDF/GNP at 0.5 wt% (e) and PVDF/GNP at 0.7 wt% (g); domain contrast of PFM at 10 V for neat PVDF (b), PVDF/GNP at 0.3 wt% (d), PVDF/GNP at 0.5% (f) and PVDF/GNP at 0.7 wt% (h).

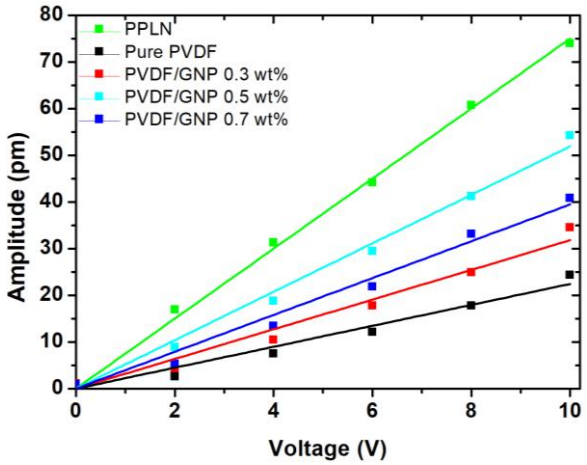

Figure 6 Measured piezoelectric signal, averaged over the 19 areas, versus the amplitude of the applied a.c. voltage.

where A_{piezo} is the amplitude of the measured piezoresponse of the calibration sample, measured in volt, and V_{ac} is the applied voltage. We then apply again Eq. (3) in order to estimate the value of d_{33} of the sample under test, using the value of ξ, obtained from Eq. (3) applied to the calibration sample, and the A_{piezo} value measured for the sample under test over an area of (500x500) nm^2, corresponding to the amplitude of the applied a.c. voltage V_{ac} [22]. The obtained d_{33} values are reported in Table 3.

Table 3 Piezoelectric coefficient evaluated by averaging the PFM signal over 19 areas each of (500x500) nm^2.

Sample	d_{33} (pm/V)
Neat PVDF	2.24 ± 0.75
PVDF/GNP 0.3 wt%	3.18 ± 1.46
PVDF/GNP 0.5 wt%	5.19 ± 1.49
PVDF/GNP 0.7 wt%	3.95 ± 1.33

We found an increase of the piezoelectric effect in the PVDF/GNP composites with respect to the neat PVDF. To correlate the piezoelectric coefficient with the presence of the β-phase in the samples, we reported d_{33} vs F(β) in Fig.7.

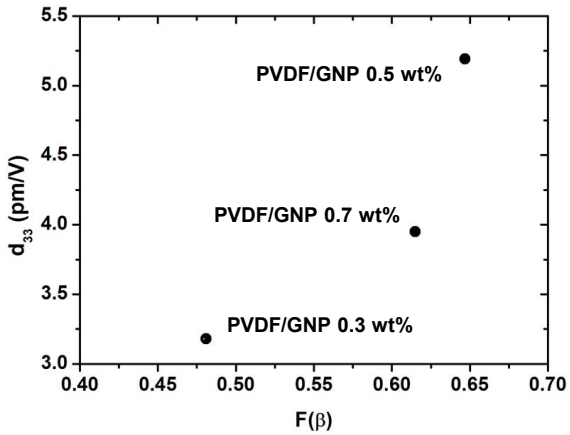

Figure 7 Averaged piezoelectric coefficient, d_{33} vs the relative fraction of the β-phase, F (β).

As we can see from Fig. 7, the piezoelectric coefficient of the PVDF/GNP nanocomposite films increases as the relative fraction of β-phase in the sample rises. This result is expected, since the electroactive β-phase determines the piezoelectric response, and is in agreement with what already reported for PVDF films [23]. On the other hand, the β-phase relative fraction does not show a monotonous behavior with GNP's concentration (see Table 2). Further investigations are ongoing to clarify the reason for this behavior. We note that the value of d_{33} for the PVDF/GNP nanocomposites investigated in this work are comparable with those reported for PVDF films filled with multiwalled carbon nanotubes (MWCNT) undrown and poled [24]. This confirms that our PVDF/GNP nanocomposites are particularly interesting, as they can provide similar d_{33} values but without poling.

Concerning the neat PVDF piezoelectric response, although it presents a high concentration of β-phase, it

shows a low value of piezoelectric coefficient. A possible reason for this behavior, could be the different fabrication process (absence of sonication) if compared to the PVDF/GNP nanocomposites.

IV. Conclusion

We presented a novel approach to increase the piezoelectric coefficient of PVDF, avoiding the poling process, by inducing an increased β-phase fraction in the PVDF film by adding to the nanocomposite opportune quantities of GNPs. Using a simple casting process of the PVDF/GNP nanocomposite, we compared the piezoelectric response of different samples: neat PVDF, PVDF nanocomposite filled with GNP at 0.3 wt%, 0.5 wt% and 0.7 wt%. The enhancement of the piezoelectric response of the PVDF / GNP nanocomposite can be explained assuming that GNPs affect on polymer structure to help the β-phase formation in PVDF, as shown elsewhere [11], [116], [167].

The results of this study show a qualitative correlation between induced β-phase, as assessed through FT-IR measurements, and intensity of the measured piezoelectric response, resulting from the PFM analysis. In fact, the obtained PFM data show the local value of the piezoelectric coefficient, measured over the sample surface in 19 spots having dimension of (500x 500) nm^2. Therefore, the obtained results demonstrate the piezoelectricity induced by the presence of a β-phase, which is induced in the nanocomposite without modification or functionalization of the GNP nor through the application of a strain or an electric field during the synthesis.

The next step of this study will be to investigate the correlation between β-phase formation and piezoelectric response, through a large-area PFM characterization of the sample surface in order to assess the uniformity of the piezoelectric response of the produced composites over the sample surface.

The obtained results can be very attractive for the fabrication at low processing temperatures of energy harvesting devices or pressure sensors on flexible substrates, avoiding chemical modification or poling.

References

[1] J. Li, S. I. Seok, B. Chu, F. Dogan, Q. Zhang, and Q. Wang, "Nanocomposites of ferroelectric polymers with TiO_2 nanoparticles exhibiting significantly enhanced electrical energy density," *Adv. Mater.*, no. 21, p. 217, 2009.

[2] G. W. Taylor, J. R. Burns, S. M. Kammann, W. B. Powers, and T. R. Welsh, "The energy harvesting eel: A small subsurface ocean/river power generator," *IEEE J. Oceanic Eng.*, no. 26, 2001.

[3] J. Granstrom, J. Feenstra, H. A. Sodano, and K. Farinholt, "Energy harvesting from a backpack instrumented with piezoelectric shoulder straps," *Smart Mater. Struct.*, no. 16, 2007.

[4] D. Mandal, K. Henkel, and D. Schmeißer, "The electroactive β-phase formation in poly(vinylidene fluoride) by gold nanoparticles doping," *Mater. Lett.*, no. 73, pp. 123–125, 2012.

[5] P. Sajkiewicz, A. Wasiak, and Z. Goclowski, "Phase transitions during stretching of poly (vinylidene fluoride)," *European polymer journal*, no. 35(3), pp. 423–429, 1999.

[6] J. Scheinbeim, C. Nakafuku, B. A. Newman, and K. D. Pae, "High–pressure crystallization of poly (vinylidene fluoride)," *Journal of Applied Physics*, no. 50(6), pp. 4399–4405, 1979.

[7] R. Miller and J. Raisoni, "Single crystals of poly (vinylidene fluoride)," *Journal of Polymer Science: Polymer Physics Edition*, no. 14(12), pp. 2325–2326, 1976.

[8] J. Luongo, "Far–infrared spectra of piezoelectric polyvinylidene fluoride," *Journal of Polymer Science Part A–2: Polymer Physics*, no. 10(6), pp. 1119–1123, 1972.

[9] V. Sencadas, R. Gregorio Jr., and S. Lanceros-Méndez, "Processing and characterization of a novel nonporous poly(vinilidene fluoride) films in the βphase," *J. Non-Cryst. Solids*, vol. 352, no. 2226, 2006.

[10] S. Manna and A. Nandi, "Piezoelectric β polymorph in poly (vinylidene fluoride)-functionalized multiwalled carbon nanotube nanocomposite films," *The Journal of Physical Chemistry C*, no. 111(40), pp. 14670–14680, 2007.

[11] R. Layek, S. Samanta, D. P. Chatterjee, and A. K. Nandi, "Physical and mechanical properties of poly (methyl methacrylate)-functionalized graphene/poly (vinylidine fluoride) nanocomposites: Piezoelectric β polymorph formation," *Polymer*, no. 51(24), pp. 5846–5856, 2010.

[12] J. Yu and et al., "Graphene nanocomposites based on poly (vinylidene fluoride): structure and properties," *Polymer Composites*, no. 32(10), pp. 1483–1491, 2011.

[13] H. Sturm, W. Stark, V. Bovtoum, and E. Schulz, "Methods for simultaneous measurements of topography and local electrical properties using scanning force microscopy," in *9th International Symposium on Electrets*, pp. 223–228, 1996.

[14] E. Soergel, "Piezoresponse force microscopy (pfm)," *J. Phys. D: Appl. Phys.*, vol. 44, p. 464003, 2011.

[15] G. De Bellis, A. Tamburrano, A. Dinescu, M. L. Santarelli, and M. S. Sarto, "Electromagnetic properties of composites containing graphite nanoplatelets at radio frequency," *Carbon*, no. 49(13), pp. 4291–4300, 2011.

[16] H. Bidsorkhi, A. D'Aloia, G. De Bellis, A. Proietti, A. Rinaldi, M. Fortunato, P. Ballirano, M. Bracciale, M. Santarelli, and M. Sarto, "Nucleation effect of unmodified graphene nanoplatelets on pvdf/gnp film composites," *Materials Today Communications*, vol. 11, pp. 163–173, 2017.

[17] C. R. Chandraiahgari, A. De Bellis, G. Martinelli, A. Bakry, A. Tamburrano, and M. Sarto, "Nanofiller induced electroactive phase formation in solution derived poly(vinylidene fluoride) polymer composites," in *IEEE International Conference on Nanotechnology*, 2015.

[18] S. Garain, T. Sinha, P. Adhikary, K. Henkel, S. Sen, S. Ram, C. Sinha, D. Schmeiber, and D. Mandal, "Self-poled transparent and flexible uv light-emitting cerium complex-pvdf composite: a high-performance nanogenerator," *ACS Appl. Mater. Interfaces*, no. 7, 2015.

[19] M. Dipankar, H. Karsten, and S. Dieter, "The electroactive β-phase formation in poly(vinylidene fluoride) by gold nanoparticles doping," *Materials Letters*, no. 73, pp. 123–125, 2012.

[20] R. Gregorio and M. Cestari, "Effect of crystallization temperature on the crystalline phase content and morphology of poly(vinylidenefluoride).," *Journal of Polymer Science Part B: Polymer Physics*, vol. 32, p. 859, 1994.

[21] J. S. Nunes, A. Wu, J. Gomes, V. Sencadas, P. M. Vilarinho, and S. Lanceros-Mendez, "Relationship between the microstructure and the microscopic piezoelectric response of the α- and β-phases of poly(vinylidene fluoride)," *Appl. Phys. A*, no. 95, pp. 875–880, 2009.

[22] D. Denning, J. Guyonnet, and B. J. Rodriguez, "Applications of piezoresponse force microscopy in materials research: from inorganic ferroelectrics to biopiezoelectrics and beyond," *International Materials Reviews*, vol. 61, 2016.

[23] J. Gomes, J. Nunes, V. Sencadas, and S. Lanceros-Mendez, "Influence of the β-phase content and degree of crystallinity on the piezo- and ferroelectric properties of poly(vinylidenefluoride)," *Smart Mater. Struct.*, vol. 19, p. 065010, 2010.

[24] G. Kim, S. Hong, and Y. Seo, "Piezoelctric properties of poly(vnylidene fluoride) and carbon nanotube blends: β-phase develpment," *Phys. Chem. Chem. Phys.*, vol. 11, pp. 10506–10512, 2009.